RESEARCH ARTICLE | SEPTEMBER 01 2024

Enhanced luminescence of oxygen atoms in solid molecular nitrogen nanoclusters [REE]

O. Korostyshevskyi 🗷 📵 ; C. K. Wetzel 💿 ; D. M. Lee; V. V. Khmelenko 📵



Low Temp. Phys. 50, 722–732 (2024) https://doi.org/10.1063/10.0028138









Enhanced luminescence of oxygen atoms in solid molecular nitrogen nanoclusters

Cite as: Fiz. Nizk. Temp. 50, 806-816 (September 2024); doi: 10.1063/10.0028138 Submitted: 20 July 2024









O. Korostyshevskyi, a) D. K. Wetzel, D. M. Lee, and V. V. Khmelenko



AFFILIATIONS

Department of Physics and Astronomy, Institute for Quantum Science and Engineering, Texas A&M University College Station, TX 77843, USA

^{a)}Author to whom correspondence should be addressed: korostyshevskyi⊚tamu.edu

ABSTRACT

We studied luminescence accompanied an injection of the nitrogen-helium gas mixture after passing discharge into dense cold helium gas. Initially, when the experimental beaker was filled with superfluid helium and the nitrogen-helium gas was injected into bulk superfluid helium at $T \approx 1.5$ K, the dominant band in the emission spectra was the α -group of nitrogen atoms. At these conditions, the nanoclusters of molecular nitrogen with high concentrations of stabilized nitrogen atoms were formed. When superfluid helium was evaporated from the beaker and the temperature at the bottom of the beaker was increased to $T \approx 20$ K, we observed a drastic change in the luminescence spectra. The β-group of oxygen atoms was dominated in the luminescence spectra, and the emission of the α-group became small. At highe temperatures ($T \approx 20 \text{ K}$), most of the nitrogen atoms recombine on the surface of N_2 nanoclusters with the formation of excited nitrogen molecules. We explained the effect of the enhancement of β-group emission by effective energy transfer from excited nitrogen molecules to the stabilized impurity oxygen atom inside N₂ nanoclusters. 2024 22:24:12

Published under an exclusive license by AIP Publishing. https://doi.org/10.1063/10.0028138

1. INTRODUCTION

The first investigations of luminescence of solid nitrogen bombarded by electrons, protons, and X-rays were carried out in 1924 by Vegard.^{1,2} These experiments aimed to provide evidence for his idea that the auroral spectrum can be explained by emission from clusters of solid nitrogen. He found that most of the auroral spectral lines can be explained by the emission of nitrogen molecules and ions. He also made an assignment of the intense auroral green line at $\lambda = 5577$ Å to the emission of the solid nitrogen exposed by electrons. Later McLennan et al.^{3,4} repeated Vegard's experiments and showed that green emission from solid nitrogen bombarded by electrons in this spectral range represented a broad band with three maxima at $\lambda = 5556$, 5617, and 5654 Å, none of each coincides with the auroral line at $\lambda = 5577$ Å. In the following work, McLennan's group observed in the laboratory emission at $\lambda = 5577 \text{ Å}$ from the discharge in gas mixtures of oxygen and rare gases (RG). This emission was assigned to the forbidden transition ${}^{1}S \rightarrow {}^{1}D$ of oxygen atom in the gas phase. 5,6

In 1950, researchers became interested in studying the luminescence of solid nitrogen for the second time when a program aimed to achieve high concentrations of stabilized atoms in solid matrices at low temperatures was initiated. Although the program's main goal of attaining high concentrations of stabilized radicals for practical applications was not achieved, comprehensive studies of the properties of various matrix-isolated species were conducted. Among them were oxygen atoms in solid molecular nitrogen. During nitrogen gas discharge products condensation onto cold surfaces (at a temperature of approximately 4.2 K), and during the bombardment of solid nitrogen by electrons, a bright green emission was observed. The most intense luminescence was registered at approximately 523 and 560 nm wavelengths. These emissions were assigned to the nitrogen atom ${}^2D \rightarrow {}^4S$ transition (so-called α -group) and to the oxygen atom ${}^{1}S \rightarrow {}^{1}D$ transition (so-called β -group), correspondingly. 8-11 Usually, in the experiments with solid nitrogen, only trace amounts (1-10 ppm) of oxygen were present. However, due to the significantly lower radiation lifetime of O (${}^{1}S \rightarrow {}^{1}D$) transition in solid N₂ matrix ($\tau_{\beta} = 0.2 \text{ ms}$)¹⁰ compared to that of N($^2D \rightarrow ^4S$) transition $(\tau_{\alpha} \approx 25-37 \text{ s})^{8,12,13}$ even small contamination of oxygen in solid molecular nitrogen provide bright emission from oxygen atoms, comparable with the emission of nitrogen atoms. Recently the radiation effects and relaxation process in pre-irradiated by an electron beam solid N₂ and N₂ doped solid RG matrix have been studied. 14-20 It was found that at low temperatures, the thermoluminescence of pre-irradiated solids

occurs due to neutralizations of ions produced during pre-irradiation by detrapping electrons, while at temperatures $T \geq 20$ K, the neutral atom diffusion and their recombination become important. The emission of oxygen atom β -group was observed in this works. ^{14–20} Strong evidence for the observation of tetranitrogen cation N_4^+ was obtained in this work Ref. 17, 18, and 20.

The third time, the emission of the β -group of oxygen atoms attracted researchers' attention during studies of the molecular nitrogen nanoclusters immersed in superfluid 4He (He II). The collections of molecular nitrogen nanoclusters, with stabilized nitrogen and oxygen atoms, were formed by injection into bulk superfluid helium of the mixture of helium gas and molecular nitrogen gas after passing the region of radio-frequency discharge. Spectra taken during sample preparation shows the most intense luminescence from stabilized nitrogen atoms at $\lambda\approx522$ nm (α -group) and oxygen atoms at $\lambda\approx560$ nm (β -group). In these experiments, oxygen was never intentionally added to the nitrogen-helium mixture, but it was present due to the small contamination of oxygen (1–10 ppm) in high-purity helium gas used in the experiments.

The strong emission of oxygen atoms β-group, accompanied by less intense β' and β'' -groups, was also observed during the destruction of impurity-helium condensates containing high concentrations of stabilized nitrogen atoms. 16,26-32 The destruction of impurityhelium condensates is accompanied by a rapid release of chemical energy stored in the samples. Interestingly, a substantial part of the stored energy is released through the emission of oxygen atoms surrounded by nitrogen molecules in the solid phase. The emissions of oxygen atoms β-group were also observed in the impurity-helium samples immersed in bulk superfluid helium during samples warming up from 1.3 to 2.16 K. 33,34 This thermoluminescence of the nanoclusters in He II is explained by recombination reactions of nitrogen atoms residing on the surfaces of nanoclusters initiated by quantum vortices in superfluid helium. Later, rotationally induced luminescence of nanoclusters immersed in He II was studied.³⁵ The β-group of oxygen atoms was always present in the luminescence spectra.

In this work, we discovered a phenomenon of enhanced luminescence of β -group of oxygen atoms in solid molecular nitrogen nanoclusters during condensation of helium-nitrogen gas jet onto a cold quartz surface. We studied the condensation of a nitrogen-helium gas jet into a beaker filled with superfluid helium. During the experiment, the supply of He II to the beaker was turned off. After the jet evaporated liquid helium from the beaker, we observed an explosion of the accumulated in the He II nitrogen-helium condensate. Soon after, the spectra maximum rapidly shifts from 522 nm (which corresponds to α -group of nitrogen) to ≈ 560 nm (β -group of oxygen), and the green β -group emission starts at a temperature around 20 K (measured by the thermometer at the bottom of the beaker) and lasts until the temperature in the beaker reaches 36 K. We will discuss the nature and the characteristics of this enhanced emission of oxygen atoms.

2. EXPERIMENTAL SETUP

The schematic of the experimental setup is shown in Fig. 1. The experimental setup consists of two concentric glass Dewars, shown as (8) and (9) in Fig. 1. The helium Dewar is filled with liquid helium. Helium vapors are pumped with an Edward 80

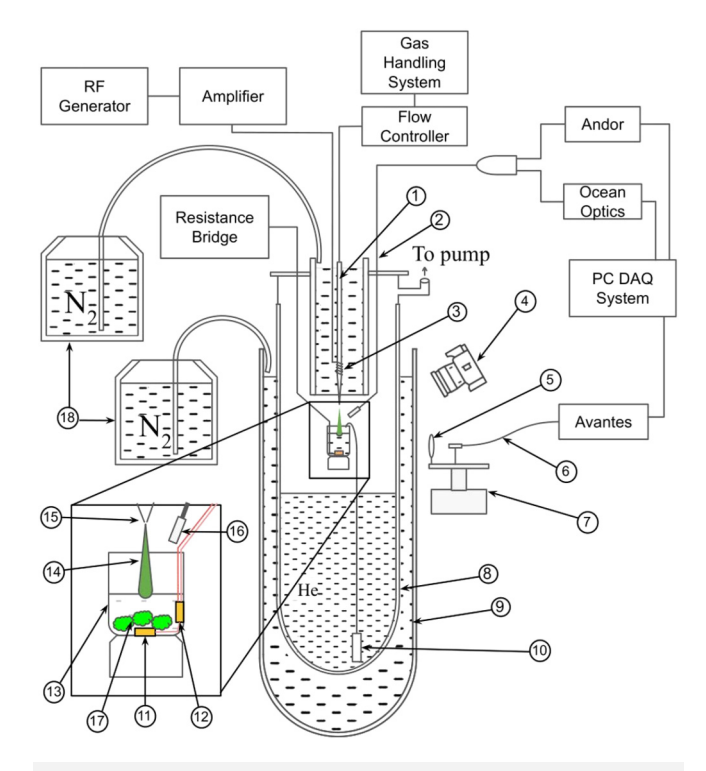


FIG. 1. Schematic of the experimental setup for the optical study of the luminescence of gas jets and impurity-helium condensates: (1) quartz capillary, (2) bifurcating optical fiber, (3) RF discharge cavity, (4) digital camera, (5) convex lens, (6) optic fiber, (7) motorized lab jack, (8) liquid helium Dewar, (9) LN₂ Dewar, (10) fountain pump, (11) first thermometer, (12) second thermometer, (13) sample accumulation beaker, (14) gas jet, (15) 0.75 mm orifice, (16) bifurcating optical fiber input, (17) impurity-helium condensate, (18) LN₂ refill system.

vacuum pump until they reach a pressure range of 0.3-5.6 torr corresponding to a desired temperature range from 1.1 to 1.6 K.

The next step involves filling the beaker with He II using a fountain pump and starting the process of sample accumulation by sending the gas mixture into helium Dewar through a quartz capillary. The gas mixture used in the experiments is prepared in a gas handling system at room temperature. The set of mixtures used in the experiments includes N₂:He ratios of 1:100, 1:200, 1:400, 1:800. The duration of each experiment varies from 15 to 30 min, depending on the conditions. The high-purity helium used in the experiments did not undergo any additional purification procedures and had O2 impurities of around 1 ppm. The gas mixture passed through the discharge zone, and the discharge products entered the helium Dewar through a 0.75 mm orifice in a quartz capillary. The RF signal for discharge is generated by a Hewlett-Packard Model 8656B signal generator and sent to an E&I 3100L RF amplifier connected to an LN2 cooled RF cavity. This is a custom-built cavity with additional shielding for decreasing influence on external electronics.³⁶ The resonance frequency of the RF cavity was varied from 76.5 to 82.5 MHz. The Brooks Model 5850E Mass Flow Controller measured gas flow and kept it at 5.10^{19} particles/s.

Inside the helium Dewar, the discharge products form a jet in the cold, dense helium gas. The jet is directed to the center of the beaker filled with He II, which is installed 2 cm below the orifice (see Fig. 1).

The usual experimental procedure consisted of accumulating the sample in bulk He II inside the beaker, turning off the supply of He II in the beaker, waiting for the helium to evaporate from the beaker, and observing the explosive destruction of the accumulated sample. During one of the experiments, this procedure was changed: the fountain pump was turned off, and the jet evaporated all the He II from the beaker. As all helium evaporated, we observed a sudden change in the emissions of $\alpha\text{-}$ and $\beta\text{-}$ group. The intensity of $\beta\text{-}$ group was increased substantially, while the $\alpha\text{-}$ group intensity diminished.

All presented optical spectra were recorded simultaneously by three spectrometers. Andor (0.35 nm resolution) and Ocean Optics (1.5 nm resolution) spectrometers are connected to the bifurcating cable, the other end of which is channeled directly into the helium Dewar and aimed at the bottom of the beaker. The Andor spectrometer has 150 lines/mm grating with 500 nm blaze (maximum sensitivity region, as shown in Fig. 2) and 360–710 nm spectral acquisition range.

An Avantes spectrometer was used to record Near-infrared (NIR) data with 5 nm resolution. The spectrometer signal was recorded from outside helium and nitrogen Dewars, which were coated with silver for thermal radiation insulation, with small strips left clear for observations. We installed convex lenses along with optic fiber on a motorized lab jack. By adjusting the position of the lab jack, we could select the region in the beaker from which we collect light for NIR signal registration. Using Ocean Optics and Avantes spectrometers simultaneously allowed us to collect data in a wide range from 200 to 1650 nm. Additionally, we used an Andor spectrometer to provide a better resolution of optical spectra. The integration time for Avantes and Ocean Optics spectrometers was 150 ms, with an external synchronization trigger of 4 Hz. The Andor spectrometer had an integration time of 50 ms with a 20 Hz internal trigger. We also filmed the luminescence of the jet and the

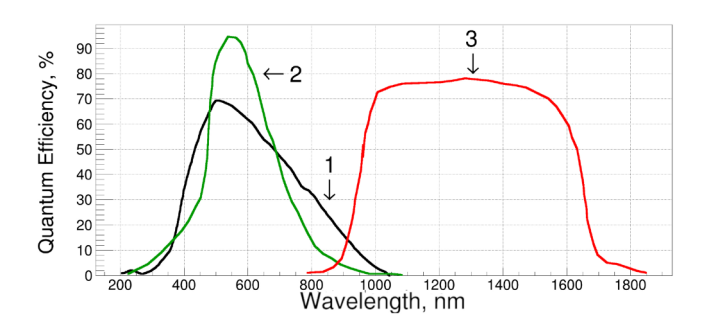


FIG. 2. Quantum efficiency as a function of wavelength of detectors used in experiments: (1) Andor Shamrock SR-500i-D2 spectrograph with SR5-GRT-0150–0500 grating (150 lines/mm, 500 nm blaze, 0.35 nm resolution) and Newton CCD (Charge Coupled Device) (black curve); (2) Ocean Optics USB2000 + spectrometer (green curve); (3) Avantes NIR512-1.7TEC spectrometer with NIR200-1.5 grating and 25 μm slit (red curve).

impurity-helium sample with a digital camera (25 mm sensor size). The camera had a lens focus of 50 mm, a shutter window of 1/100 s, an f-stop of f/4.0, a sensitivity of ISO 4000, a resolution of 720p, and a recorded video at 60 frames per second.

Two thermometers were placed inside of the beaker. The first thermometer is secured at the center, at the bottom of the beaker, and the second is placed vertically on the side of the beaker. The first thermometer is shown in Fig. 1 and Fig. 6(b). Thermometers are LakeShore germanium resistors (GR-200A series) connected to the LR-400 resistance bridge. Temperature differences between two thermometers up to 1 K were recorded (after He II evaporation). This difference is a result of different thermometers' locations.

Two automatic LN₂ refill systems control liquid nitrogen levels in the LN2 Dewar and the quartz tube, where the RF discharge cavity and the quartz capillary are located. The two refill systems are almost identical but differ only in thermocouple locations. One system consists of a thermocouple pair, HP 3478A Multimeter, microcontroller system, gas solenoid valve, pressurized nitrogen gas supply, and LN₂ refill Dewar. As soon as the LN₂ level in the main (glass) Dewar drops below the thermocouple location, it starts to heat up. The heat-up process causes a change in the potential difference at the thermocouple, which the multimeter detects. Multimeter readings changes are monitored by a microcontroller, which triggers the gas solenoid valve to open, increasing pressure in the refill LN2 Dewar. Pressure causes liquid nitrogen flow from the refill Dewar to the main one (see Fig. 1). The quartz tube refill system works the same way, the only difference being that it has two thermocouple pairs at the top and bottom of the tube and ref erence Dewar filled with LN₂.

The pressure inside the helium Dewar was monitored by and MKS gauge and recorded by the PC DAQ system.

3. EXPERIMENTAL RESULTS

Solid nitrogen nanoclusters are formed by injecting nitrogen. helium gas mixture discharge products into dense cold helium gas above the surface of He II. After entering bulk He II nanoclusters form a porous gel-like structure inside He II. Each nanocluster is covered with a few layers of solid helium, which impedes the recombination of atomic nitrogen, mostly stabilized on the nanocluster's surface. 34

Figure 3 displays the time integrated luminescence spectra of the entire observation period for the experiment conducted with a gas mixture of N_2 :He = 1:200. All identified lines are marked in the figure and listed in Table I. The bands of first $(B^3\Pi_g \to A^3\Sigma_u^+)$ and second $(C^3\Pi_u \to B^3\Pi_g)$ positive systems of molecular nitrogen, as well as atomic lines of helium, oxygen, and nitrogen, are present in the spectra. Nitrogen molecular bands and helium lines correspond to gas phase emission from the jet. Atomic α - and δ -group of the nitrogen and β-group of oxygen corresponds to the emission of atoms stabilized in solid molecular nitrogen. Despite using a mixture of N_2 :He = 1:200 and having O_2 impurities in He gas of around 1–2 ppm, the oxygen atom $\beta\mbox{-group}$ intensity is an order of magnitude higher than the nitrogen atom α -group intensity, as evident from the figure. The dynamics of the luminescence spectra, recorded by the Andor spectrometer, are presented in Fig. 4 in logarithmic scale.

2024 22:24:

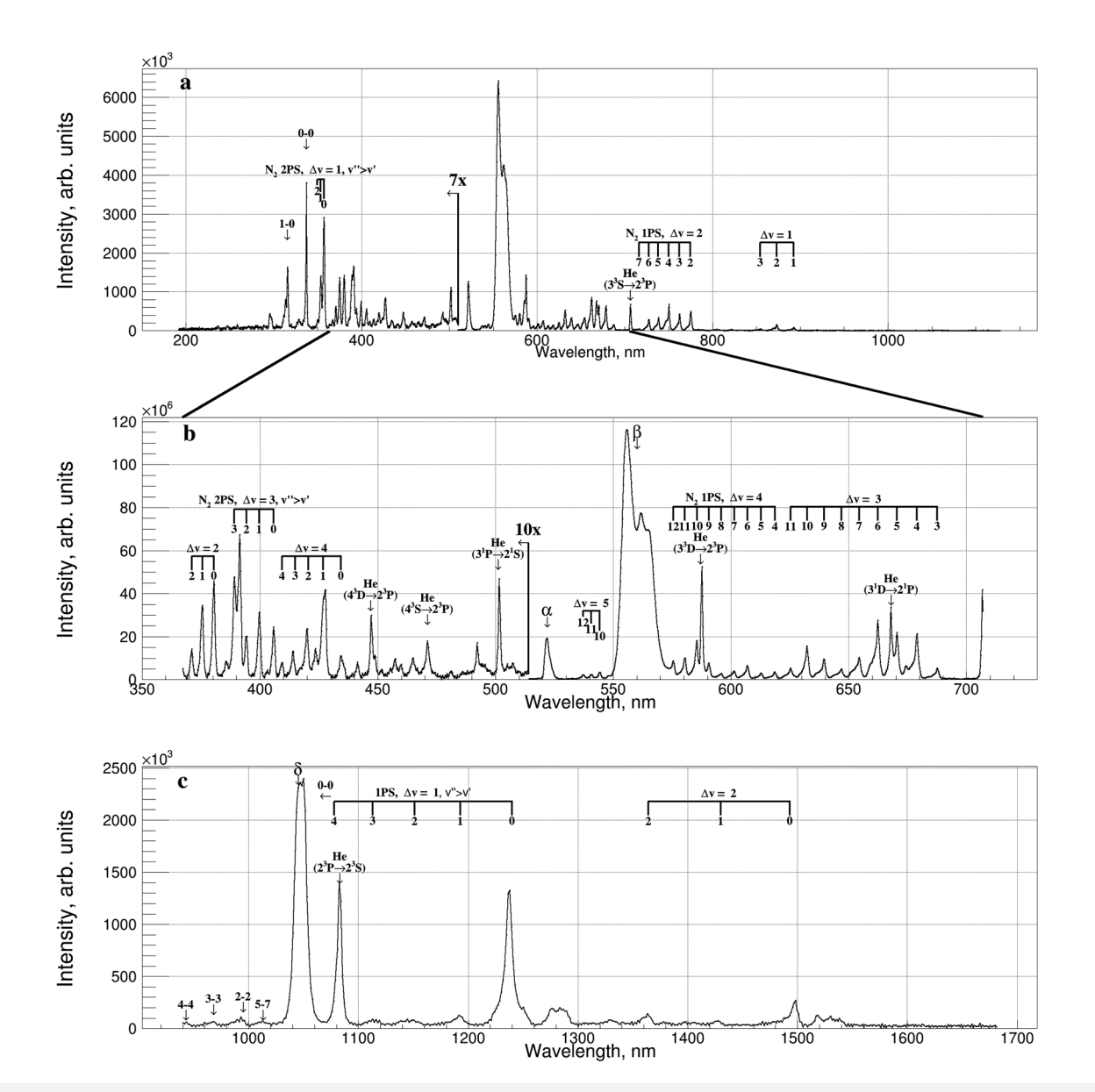


FIG. 3. Integrated spectra of luminescence, during N_2 :He = 1:200 gas mixture condensation, observed with three different spectrometers: Ocean Optics (a), Andor (b), and Avantes (c). The experiment consists of the following phases: accumulation of the sample in bulk He II, evaporation of the He II by the jet, explosive destruction of the accumulated sample, and a new regime of intense β -group emission.

We will be focusing our attention on luminescence in a range from 550 to 570 nm, which belongs to the β -group (${}^1S \rightarrow {}^1D$ transition in oxygen atom), and in a range from 520 to 525 nm, which corresponds to α -group (${}^2D \rightarrow {}^4S$ transition in nitrogen atom). The dynamics of the integrated intensities of those bands is shown in Fig. 5, alongside the temperature. Noise in the spectrum integral (see Fig. 5) can be assigned to the slight instability in the discharge.

From Fig. 5 one can see that while the helium level in the beaker was relatively high the α -group emission was stronger than

the β -group emission [see Figs. 6(a) and 6(b)], but when more and more helium was evaporated by the jet (helium supply to the beaker was terminated) the β -group emission started to be more prominent (around 300 s mark, see Fig. 5). At point c in Fig. 5, all helium was evaporated from the beaker, which led to the explosion of the accumulated sample [see Figs. 6(c) and 6(d)]. The explosive destruction period is less than one second. Intense β -group emission starts almost instantly after the liquid helium is evaporated and, therefore, synchronized with the sample explosion. If the

TABLE I. Wavelengths of the transitions for different energy levels of molecular nitrogen, atomic nitrogen, atomic oxygen, and helium, which were identified in obtained spectra.

Molecular nitrogen bands												Atomic lines and groups		
$B^3\Pi_g o A^3\Sigma_u^+(1+)$									$C^3\Pi_u \to B^3\Pi_g(2+)$			Element	Energy levels	λ, nm
v'	ν''	λ, nm	ν'	v''	λ, nm	ν'	v''	λ, nm	ν'	v''	λ, nm	Не	$4^3D \rightarrow 2^3P$	447.1
0	0	1051	3	4	1113	7	5	716.4	0	0	337.1		$4^3S \rightarrow 2^3P$	471.3
	1	1240	4	0	618.6	8	4	595.9		1	357.6		$3^1P \rightarrow 2^1S$	501.6
	2	1498		1	678.8		5	646.8		2	380.4	N	$^{2}D\rightarrow {}^{4}S(\alpha)$	≈522
1	0	891.2		2	750.4	9	5	590.6		3	405.9	O	$^{1} S \rightarrow ^{1}D(\beta)$	≈560
	1	1022		4	943.6		6	639.4		4	434.3	He	$3^3D \rightarrow 2^3P$	587.6
	2	1193		5	1078	10	5	544.2	1	2	353.6		$3^1D \rightarrow 2^1P$	667.8
	3	1430	5	1	612.7		6	585.4		3	375.5		$3^3S \rightarrow 2^3P$	706.5
2	0	775.3		2	670.4		7	632.2		4	399.8	N	$^{2}P\rightarrow ^{2}D(\delta)$	≈1040
	1	872.3		3	738.7	11	6	540.6		5	426.9	He	$2^3P \rightarrow 2^3S$	1083
	2	994.2		6	1044		7	580.4	2	3	350			
	3	1151	6	2	606.9		8	625.3		4	371			
	4	1364		3	662.3	12	7	537.2		5	394.3			
3	0	687.5		4	727.3		8	575.5		6	420			
	1	762.6		7	1013				3	6	389.4			
	2	854.2	7	3	601.3					7	414.2			
	3	968.2		4	654.5				4	8	409.4			

sample accumulation time was short, we don't have enough sample in a beaker for its explosion to be distinctive on top of the intense β-group emission regime. After the explosion, the nature of the emission, and correspondingly spectrum, changed rapidly and drastically. The α-group almost completely disappears, and β-group luminescence increases tenfold [see Fig. 6(e)]. One can visually observe how a prominent β-group emission appeared from the bottom of the beaker [see Fig. 6(f)]. We consistently recreated the observed effect multiple times. The green $\beta\mbox{-}\text{group}$ emission continued for around 500 s but became less intense with time [see Figs. 6(g) and 6(h)] and ended when the temperature on the

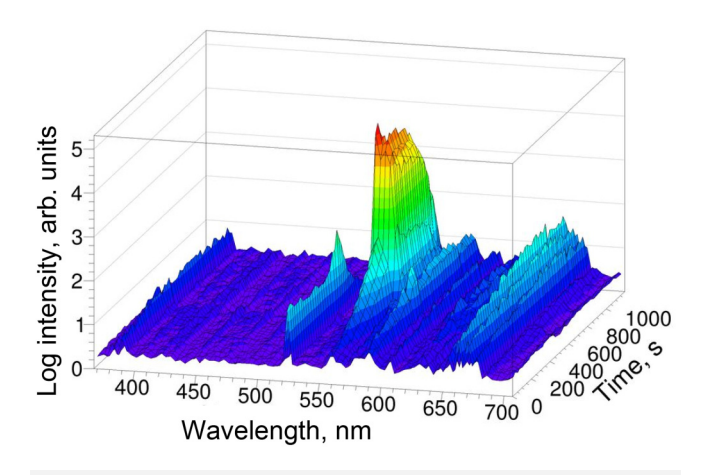


FIG. 4. Dynamics of luminescence spectra during N₂:He = 1:200 gas mixture condensation taken by Andor spectrometer with an exposure time of 50 ms.

thermometer reached $T \approx 36 \, \text{K}$. After the emission disappeared, the experiment could be continued. If the fountain pump was turned on

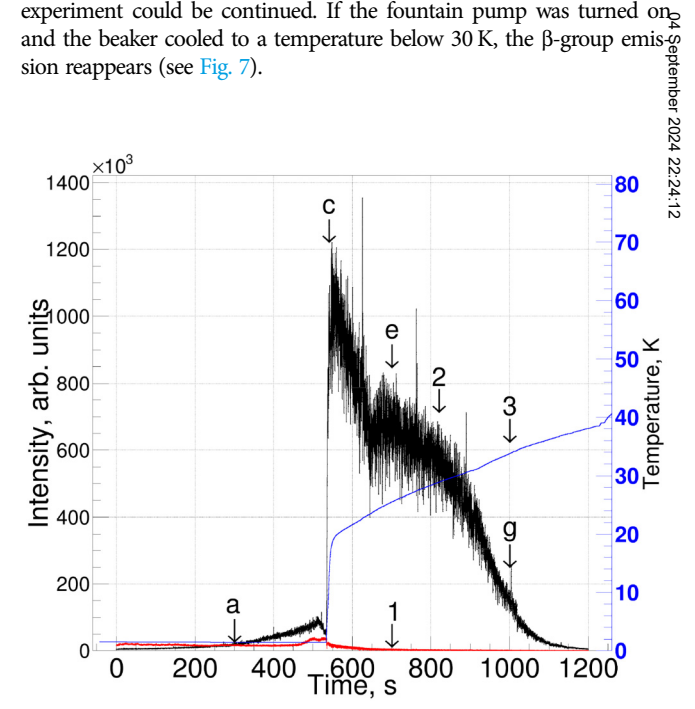


FIG. 5. Kinetics of α -group emission integral from 520 to 525 nm (1, red), β-group emission integral from 550 to 570 nm (2, black), and temperature (3, blue) during the experiment with N_2 :He = 1:200 gas mixture. Letters correspond to points in time, which are more closely inspected in Fig. 6.

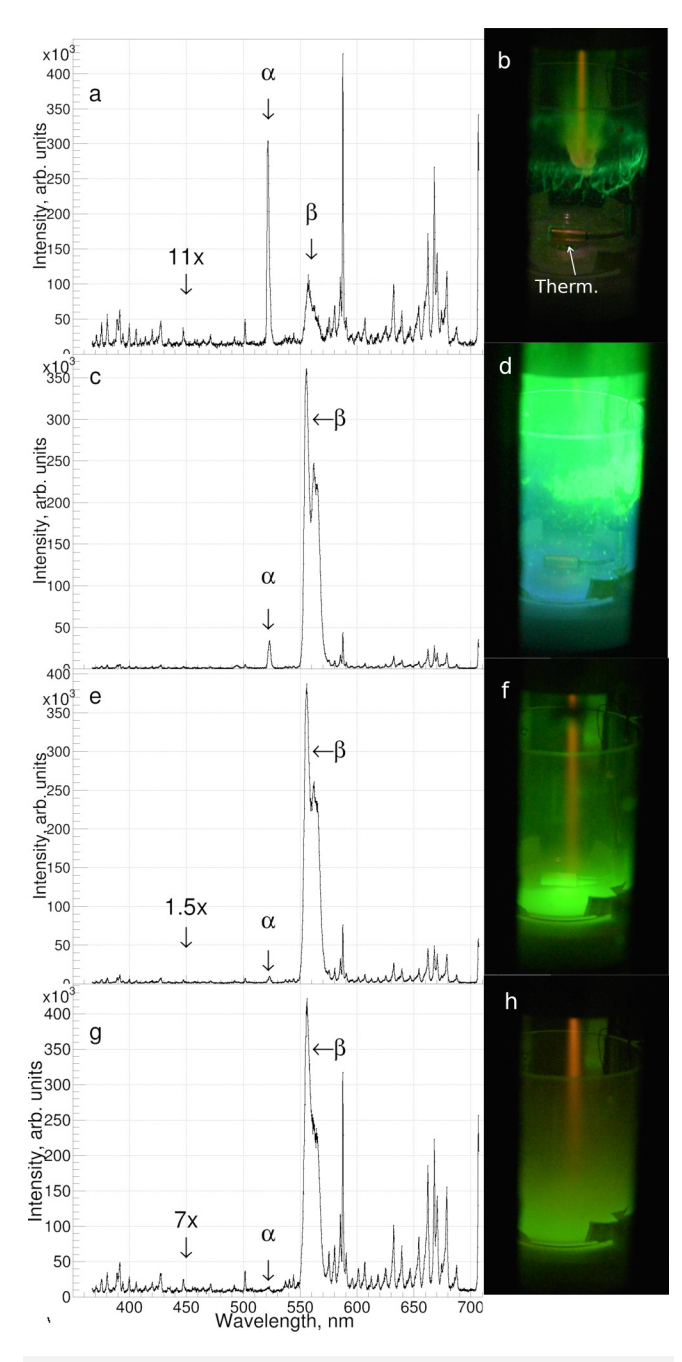


FIG. 6. Spectra of luminescence during condensation of N₂:He = 1:200 gas mixture obtained by Andor spectrometer at different moments in time and image of the jet and the sample at the same moments. Integration window is 1 s. (a), (b). At t = 300 s during sample accumulation in bulk He II phase; (c), (d) at t = 540 s during the accumulated sample explosive destruction time; (e), (f) at t = 700 s, the enhanced β-group emission period; (g), (h) at t = 1000 s, the beaker temperature reaches 36 K, and the green glow almost disappears. × 11 at (a), × 1.5 at (e), and ×7 at (d) represent amplification of the spectra along the t axis for corresponding panels.

We performed a special set of experiments to understand the possible role of the nanoclusters accumulated in He II on the observed phenomenon of enhanced emission of β -group of oxygen atoms in the collection of N_2 nanoclusters. In these experiments, with gas mixture N_2 :He = 1:200, different accumulation times were used for collection of nanoclusters in bulk He II ($t_{\rm acc}$ = 0, 5, and 10 min) before starting the evaporation process of He II from the beaker. When He II evaporated from the beaker, we observed explosive destruction for each sample. The emission intensity during sample destruction was proportional to the sample accumulation time. For each of the three experiments, we observe the effect of the enhancement of β -group emission after sample destruction. The dependence of β -group emission on temperature for three different accumulations is shown in Fig. 8.

It has been observed that a longer accumulation time has a negative impact on the luminescence intensity of the β -group but leads to higher-intensity explosions due to the larger amount of accumulated nanoclusters.

In one of the experiments, bulk He II was evaporated by the pure helium jet. When the beaker was empty, and the temperature in the beaker reached 25 K, the gas supply was switched from pure helium to the N_2 :He = 1:200 mixture, and intense β -group emission appeared in the jet and at the bottom of the beaker.

We studied the influence of nitrogen atom concentration in the gas jet on the observed enhanced β -group emission of O atoms in N_2 nanoclusters. We used N_2 –He gas mixtures with different N_2 content from 1/800 to 1/100 in these experiments. It is known that the concentration of nitrogen atoms in the discharge products of N_2 –He gas mixture is proportional to the content of N_2 molecules. Fig. 9 shows the dependence of the β -group emission integral on the content of N_2^∞ molecules in the condensing N_2 –He gas mixtures. One can see that increasing N_2 content from 1/800 to 1/200 in N_2 –He mixtures led to a linear increase of the O atoms β -group emission in N_2 nanoclusters but a further increase of N_2 content to 1/100 results in a significant drop in intensity of β -group emission.

Also, experiments with a neon-nitrogen-helium mixture were conducted. The spectra accumulated during those experiments are shown in Fig. 10. The addition of neon to the nitrogen-helium gas mixture decreases luminescence intensity from the jet and the nitrogen-neon nanoclusters.

4. DISCUSSION

Activated solid nitrogen containing stabilized nitrogen atoms exhibits a strong optical emission at low temperatures. Previous studies of N–N₂ systems include condensation of products from gaseous discharge as well as γ rays and electron bombardment of solid nitrogen. Intense "green" emissions were observed in these experiments. Most intense bands in these emissions were assigned to the forbidden transitions $^2D \rightarrow ^4S$ of nitrogen atoms and $^1S \rightarrow ^1D$ of oxygen atoms. These transitions are strongly forbidden in a gas phase. The lifetime of N ($^2D \rightarrow ^4S$) transition in gas phase is $\approx 44.5 \, \mathrm{h}^{37}$ and of O ($^1S \rightarrow ^1D$) transition is 0.75 s. 38 The N ($^2D \rightarrow ^4S$) is also forbidden by the angular momentum selection rule and the parity rule for dipole transition at centrosymmetric atomic sites in solid N₂ lattice. However, it occurs as induced dipole radiation due to

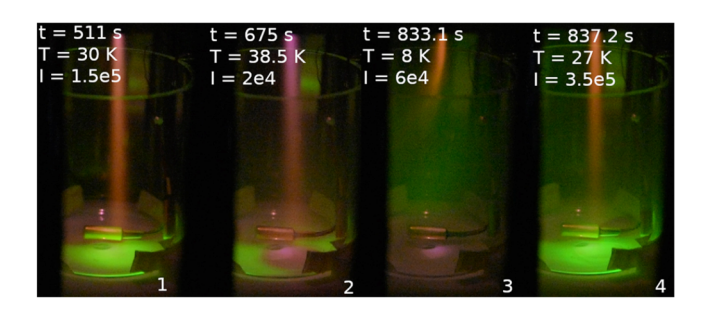


FIG. 7. Images of the jet and the β-group emission from the bottom of the beaker taken at different points in time. Time, temperature, and integral intensity of β-group (50 ms accumulation time) are shown at the top of each frame. In frame 1, one can see the usual regime after some time after the explosion. In frame 2, the bottom of the beaker (registered by the thermometer, one can see) is heated above 36 K, and the β-group emission is weak. There is no green glow in the region directly under the jet at the bottom of the beaker. In image 3, the fountain pump is turned on and starts to supply He II into the beaker. In image 4, the bottom of the beaker is cooled down, and the intensity of β emission is higher than in image 1. The gas mixture N₂:He = 1:400 was used in this experiment.

the weak dynamical perturbing fields arising from lattice vibrations. ¹² The lifetime of N atom α -emission in solid N₂ is $\approx 30 \, \mathrm{s}^{.8,12,13}$ The influence of N₂ lattice on O ($^1S \rightarrow ^1D$) transition is even stronger. This parity-forbidden oxygen transition in the N₂ lattice is composed of a group of three broad components. One component is blue-shifted, whereas the other two are red-shifted compared to the gas phase wavelength of 5577 Å. The primary trapping site for N and O atoms in the N₂ lattice is the substitutional centrosymmetric site of symmetry S₆. ^{11,16} The β -group of O atoms in this site is composed of three components due to crystal field splitting of the final O (1D_2) state. Each component contains a zero phonon line origin,

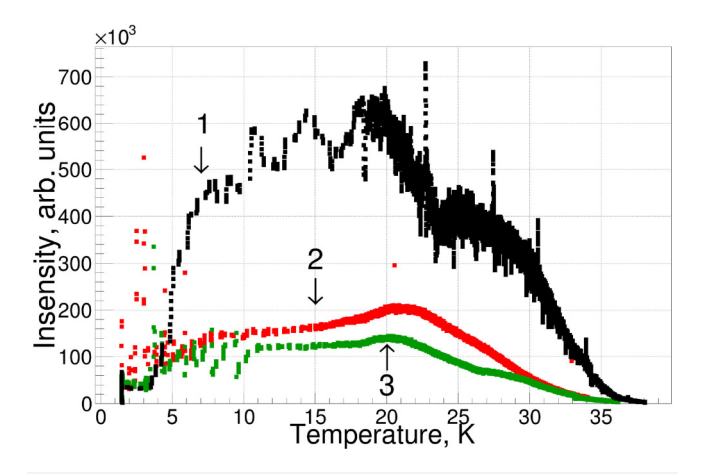


FIG. 8. Dependence of β-group intensity on temperature in the beaker. All lines correspond to the same gas mixture of N_2 :He = 1:200 but with different accumulation times before the fountain pump was turned off: (1) no accumulation (black), (2) 5 min accumulation (red), (3) 10 min accumulation (green).

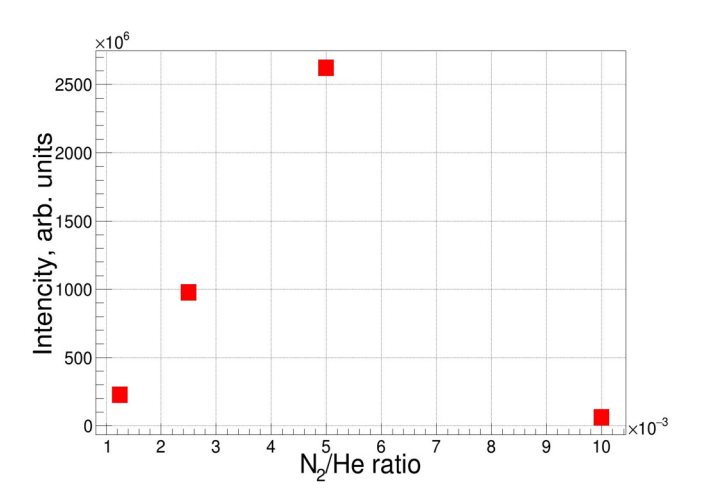


FIG. 9. Dependence of integrated O atom β-group (550–570 nm) luminescence intensity on N_2 content in condensing nitrogen-helium gas mixtures.

which gives rise a little or no emission. The asymmetric phonon-induced modes of N_2 lattice cause a change in parity, and the O (${}^1S \rightarrow {}^1D$) transition becomes dipole-allowed, resulting in the almost identical lifetimes of all three components of the β -group.

The N and O atoms excitation mechanism in solid N_2 is also well established. ^{12,49} It includes the recombination of N (⁴S) atoms and formation of metastable $N_2(A^3\Sigma_u^+)$ molecules:

$$N(^4S) + N(^4S) \rightarrow N_2(A^3\Sigma_u^+, \nu).$$

The energy of metastable molecules can be easily transferred through the N_2 matrix. When the excitation approaches the stabinary lized atoms, it transfers energy to them:

$$N_2(A^3\Sigma_u^+, \nu) + N(^4S) \to N(^2D) + N_2(X^1\Sigma_g^+, \nu'),$$

 $N_2(A^3\Sigma_u^+, \nu) + O(^3P) \to O(^1S) + N_2(X^1\Sigma_g^+, \nu')$

with the following emissions from atoms:

$$N(^2D) \rightarrow N(^4S) + \alpha$$
-group,
 $O(^1S) \rightarrow O(^1D) + \beta$ -group.

This mechanism explains emissions during the accumulation products of the discharge in N_2 gas on the cold surfaces and upon bombardment of solid N_2 by electrons and γ rays, as well as thermoluminescence accompanied by warming up of solid N_2 containing stabilized N and O atoms.

We injected the nitrogen-helium gas mixture discharge products into the bulk superfluid helium in our experimental method. On the way from the entering orifice to the surface of He II, the nanoclusters of solid N_2 , containing a high concentration of N atoms, are formed. Most of the N atoms are stabilized on the surface of nanoclusters. 36,40,41 The nanoclusters form an aerogel-

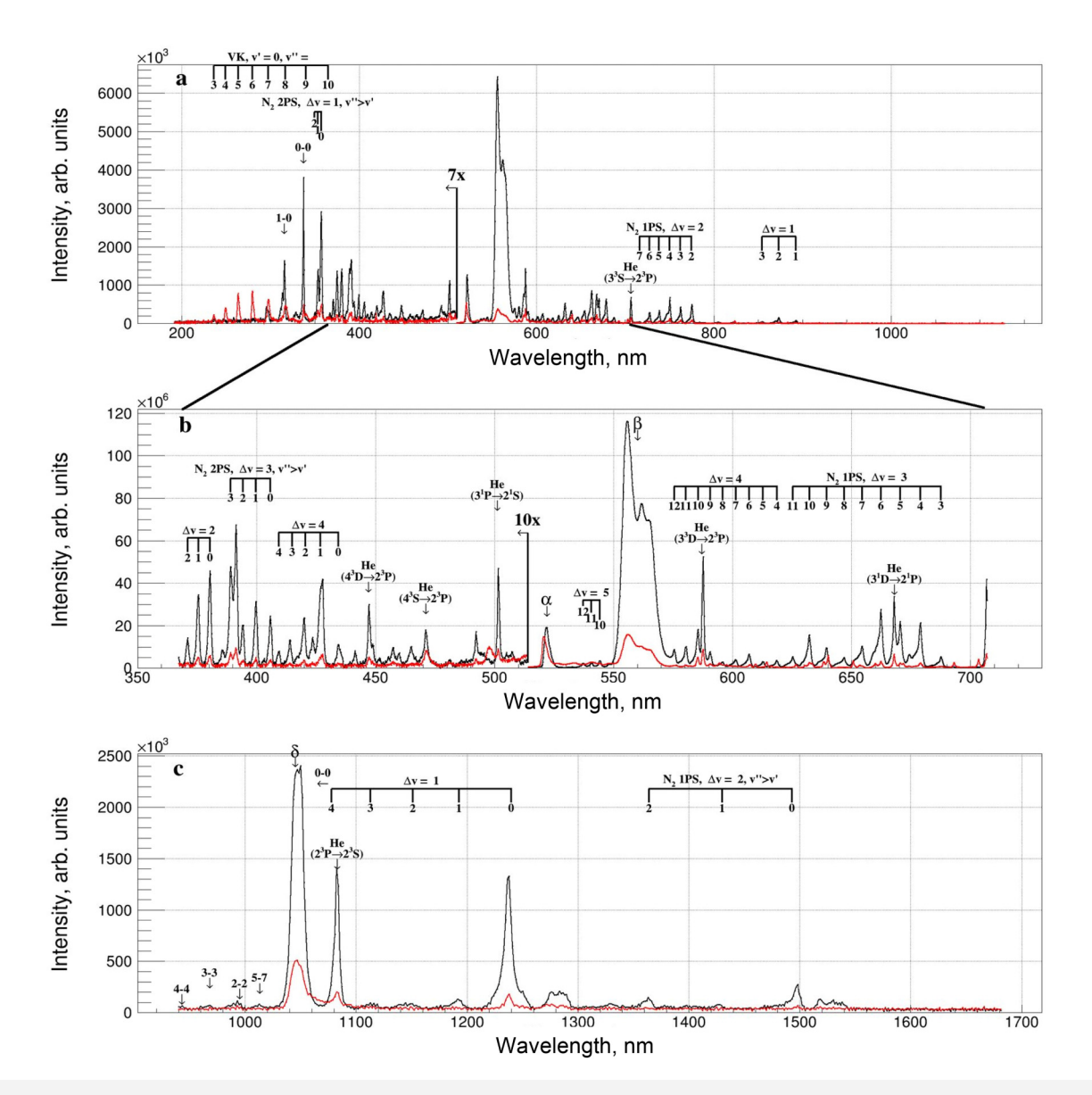


FIG. 10. Comparation of integrated spectra of the jet and the impurity-helium sample luminescence obtained by three spectrometers for experiments with N_2 :He = 1:200 (black lines) and N_2 :Ne:He = 1:5:1000 (red lines) gas mixtures. Spectra obtained by Ocean Optics (a), Avantes (b), and Andor (c) spectrometers. The regimes for obtaining integrated spectra are similar to that described in Fig. 3. In a nitrogen-neon-helium mixture, the content of nitrogen is reduced by 5 times compared to that of the nitrogen-helium mixture. This reduction led to a substantial decrease in all emissions.

like structure inside He II. $^{45-47}$ The abovementioned mechanism also explains the green luminescence of the collection of nanoclusters during accumulation. The integral of α -group emission is much larger than that of β -group emission. The expanded spectrum of β -group during sample accumulation is shown in Fig. 11(a).

The investigation of the emission spectra during the explosive destruction of the collection of the nanoclusters shows that in these fast flashes, the emission intensity of β -group is much larger than

that of α -group. The relative increase of β -group intensity was explained by reducing the concentration of stabilized atoms due to their recombination and the much smaller lifetime of the oxygen atom transition, which provides an efficient channel for releasing the energy created in the sample from the recombination of stabilized nitrogen atoms. The spectrum of β -group during sample destruction is shown in Fig. 11(b).

In this work, we described the regime of enhanced longtime β -group emission of oxygen atoms in solid molecular nitrogen

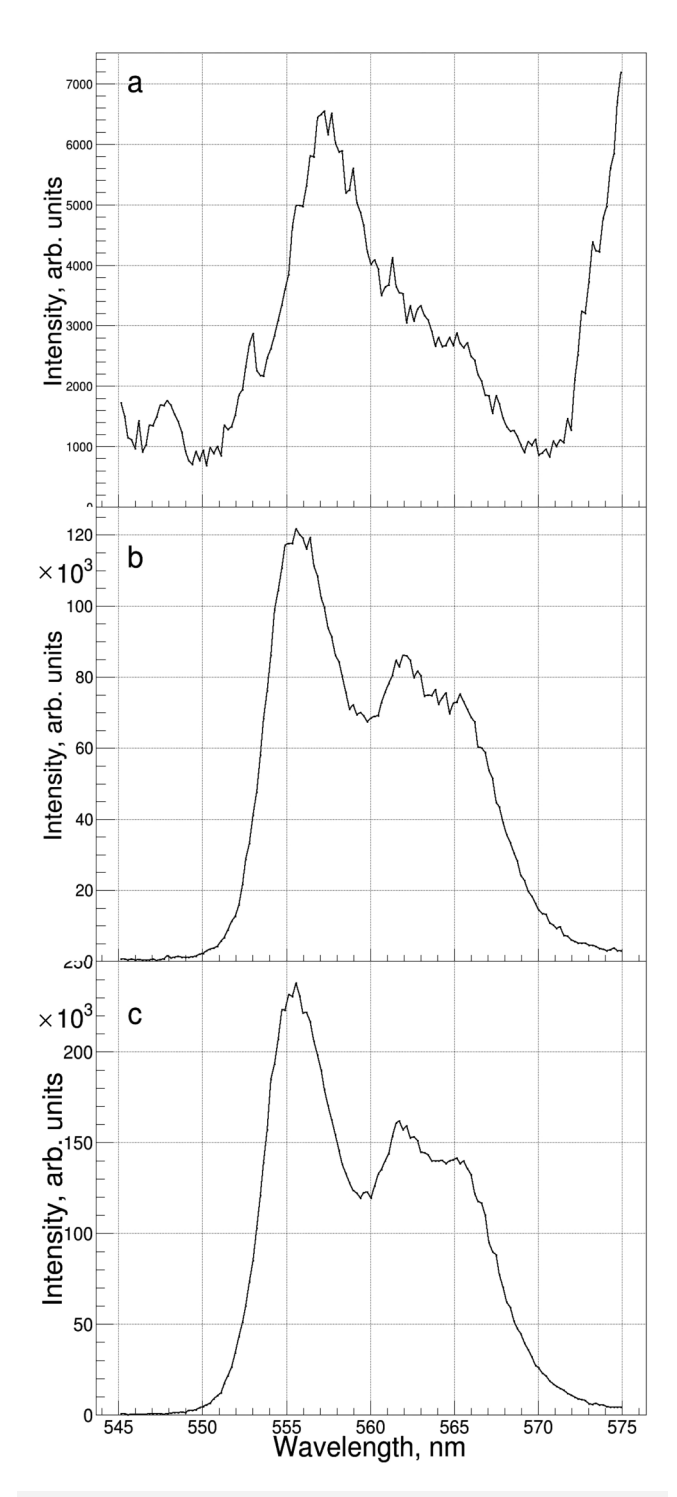


FIG. 11. Spectra of β-group luminescence during N_2 :He = 1:200 gas mixture condensation, obtained by Andor spectrometer at different moments with time integration window of 1s: (a) during sample accumulation in bulk He II at t = 300 s; (b) during the sample explosive destruction at t = 540 s; (c) during intense β-group luminescence period at t = 700 s.

nanoclusters. The regime was realized during condensation of activated (passing RF discharge) nitrogen-helium gas jet into dense cold helium gas at temperatures of 20–35 K. The spectrum of β -group during enhanced emission regime is shown in Fig. 11(c). The similarity of the β -group spectra during enhanced emission regime and that during the destruction of N_2 nanoclusters collection containing a high concentration of stabilized nitrogen atoms [see Figs. 11(b) and 11(c)] suggest the resemblance of the emission mechanism for these two cases.

The phenomenon of the enhanced oxygen atom β-group emission during nitrogen-helium gas jet condensation in a cold helium vapor can be explained by the following mechanism. The nanoclusters of molecular nitrogen are formed upon cooling down of the discharge products in the cold helium gas. The N_2 :He = 1:200 gas mixture contains 0.5% of N₂ molecules and $\approx 10^{-3}$ % of O₂ molecules. The O2 molecules appear as an impurity in the helium gas. The flux of the helium gas is $\approx 5 \cdot 10^{19} \text{ s}^{-1}$, so the flux of N₂ molecules is $dN_2/dt \approx 2.5 \cdot 10^{17} \text{ s}^{-1}$, and the flux of O_2 molecules is $\approx 5 \cdot 10^{14} \text{ s}^{-1}$. In a cold helium gas, the nanoclusters of N2 molecules with a size of $\approx 5-10 \,\mathrm{nm} \ (\approx 2500 \,\mathrm{N}_2 \,\mathrm{molecules})$ are formed. The rate of cluster formation is $dn_{\rm cl}/dt \approx 1 \cdot 10^{14} {\rm s}^{-1}$. Therefore, the N₂ nanoclusters formation rate is of the same order as the flux of O2 molecules. At such a small content of O2 molecules in the He gas, all O2 molecules are dissociated in the discharge zone.⁴⁸ Therefore, only the atomic form of oxygen should be present in the gas jet. These O atoms might be at the center of nanoclusters. The mechanism of stabilizing O atoms in the interior of N2 nanoclusters involves recombination with N atoms, resulting in the formation of NO molecules. Because of a large van der Waals attraction, NO molecules can beg centers of N₂ nanoclusters formation. When the NO molecule attracts an N atom, a fast reaction NO+N \rightarrow N2+O results in stabilizing the O atom surrounded by N₂ molecules. As a result, each N₂ nanocluster should have a few (up to 5) O atoms stabilized in the interior. of N₂ nanoclusters. In the usual conditions at temperatures of $\approx 1.5 \text{ K}$, N atoms mostly stabilized on the surfaces of N₂ nano- N clusters. 36,40,41 In the condition of observation of intense β emission of O atoms in N2 nanoclusters, the temperature is much higher (≈24-35 K), and at high temperature, the efficiency of stabilization became much smaller, and N atoms from the jet mostly recombine on the surfaces of nanoclusters formed in the peripheral cold region of the jet. The metastable N_2 $(A^3\Sigma_u^+)$ molecules formed on surfaces of N₂ nanoclusters transfer excitation energy into the interior of nanoclusters, where O (3P) atoms are stabilized. The fast energy transfer through N2 molecules in nanoclusters delivers energy for the excitation of stabilized O atoms in N2 nanoclusters.4

The relatively short lifetime of O (${}^1S \rightarrow {}^1D$) transition (≈ 0.2 ms), comparative to the ≈ 30 s for N (${}^2D \rightarrow {}^4S$) transition, provides an efficient channel of emission β -group of O atoms. The large surface area of the collection of nanoclusters makes the process of recombination of N atoms very effective, and most of the chemical energy from the excited N₂ molecules is released as an emission of oxygen atoms. Much less intensity of α -group of N atoms was observed in this regime as seen in Figs. 6(e) and 6(g).

We did not observe any bands of O_2 molecules or O_2^+ ions in the experimental spectra. With low concentrations of O atoms, the probability of their recombination is very small. Also, there is no

evidence for the influence of charge recombination reactions on the observed phenomenon of enhanced $\beta\text{-}group$ emission of O atom in N_2 nanoclusters.

The results presented in Fig. 9 show the dependence of β -group emission of O atoms, stabilized in N_2 nanoclusters, on the N_2 content in N_2 -He gas mixture. Higher nitrogen molecule content in the gas mixture leads to larger nitrogen atom concentration in the discharge products, resulting in increased nitrogen atom recombination rate on the surface of the nanoclusters, providing higher energy flux for excitation of O atoms stabilized in N_2 nanoclusters. Since stabilized oxygen provides an efficient energy release channel through the $^1S \rightarrow ^1D$ transition, we see an increase in β -group luminescence intensity. The intensity of β -group emission is linearly growing with increasing content, from 1/800 to 1/200, of N_2 molecules in the N_2 -He gas jet. However, when the energy flux is too large, the nanoclusters are melted, and the β -emission almost disappears, as observed for the 1/100 content of N_2 molecules in N_2 -He gas jet.

The suggested mechanism is supported by an experiment with the addition of Ne atoms to the N2:He gas mixture. The gas mixture change from N_2 :He = 1:200 to N_2 :Ne:He = 1:5:1000 is a 5-time reduction in nitrogen content, which leads to substantial suppression of the intensity of all emissions (see Fig. 10). The presence of Ne atoms also changes the structure of nanoclusters. Neon atoms are captured in the interior and on the surfaces of N2 nanoclusters. 6 In this case, the N atoms from the jet recombine on the surface of nanoclusters with the formation of excited N2 molecules. However, the Ne atoms suppress the transfer of excitation from the N₂ molecules on the surface to the interior of N₂ nanoclusters, since the lowest excited state of Ne atom (≈16.6 eV) is much higher than the energy released in N (4S) atom recombination (\approx 9.8 eV).²⁴ Therefore, the emission of β-group of O atoms inside the N₂ nanoclusters is substantially suppressed, as observed in experiments with the gas mixture containing neon.

5. CONCLUSIONS

We observed enhanced β -group emission of oxygen atoms in the collection of molecular nitrogen nanoclusters at temperatures of 20–35 K. The energy for excitation of O (3P) atoms was transferred through the N_2 matrix from the surface of nanoclusters. This energy results of the recombination of N atoms from the gas jet on the surfaces of N_2 nanoclusters, leading to the formation of the metastable N_2 ($A^3\Sigma_u^+$) molecules. The fast process of excitation transfer through the N_2 matrix and the relatively small lifetime of O ($^1S \rightarrow ^1D$) transition provide an efficient mechanism of enhanced luminescence of oxygen atoms in solid molecular nitrogen nanoclusters.

ACKNOWLEDGMENTS

This work was supported by NSF grant DMR 2104756.

REFERENCES

- ¹L. Vegard, Nature 113, 716 (1924).
- ²L. Vegard, Nature 114, 357 (1924).
- ³G. M. Shrum and J. C. McLennan, Proc. R. Soc. (London) A **106**, 138 (1924).
- ⁴J. C. McLennan, Nature 115, 46 (1925).

- ⁵J. C. McLennan and G. M. Shrum, Proc. R. Soc. (London) A 108, 501 (1925).
- ⁶J. C. McLennan, Proc. R. Soc. (London) A **120**, 327 (1928).
- ⁷A. M. Bass and H. P. Broida, Formation and Trapping of Free Radicals (Academic Press, New York, 1960).
- ⁸A. M. Bass and H. P. Broida, Phys. Rev. **101**, 1740 (1956).
- ⁹M. Peyron and H. P. Broida, J. Chem. Phys. **30**, 139 (1959).
- ¹⁰E. M. Hörl, J. Mol. Spectrosc. **3**, 425 (1959).
- ¹¹R. J. Sayer, R. H. Prince, and W. W. Duley, Phys. Status Solidi B **106**, 249 (1981).
- ¹²O. Oehler, D. A. Smith, and K. Dressler, J. Chem. Phys. **66**, 2097 (1977).
- ¹³R. J. Sayer, R. H. Prince, and W. W. Duley, Proc. R. Soc. (London) A 365, 235 (1979).
- ¹⁴A. N. Ponomaryov, E. V. Savchenko, I. V. Khyzhniy, G. B. Gumenchuk, M. Frankowski, and V. E. Bondybey, Fiz. Nizk. Temp. **33**, 705 (2007) [Low Temp. Phys. **33**, 532 (2007)].
- ¹⁵E. V. Savchenko, I. V. Khyzhniy, S. A. Uyutnov, G. B. Gumenchuk, and A. N. Ponomaryov, IOP Conf. Ser. Mater. Sci. Eng. 15, 012082 (2010).
- ¹⁶R. E. Boltnev, I. B. Bykhalo, I. N. Krushinskaya, A. Pelmenev, V. V. Khmelenko, D. M. Lee, I. V. Khyzhniy, S. A. Uyutnov, E. V. Savchenko, A. N. Ponomaryov, G. B. Gumenchuk, and V. E. Bondybey, Fiz. Nizk. Temp. 39, 580 (2013) [Low Temp. Phys. 39, 451 (2013)].
- ¹⁷E. V. Savchenko, I. V. Khyzhniy, S. A. Uyutnov, A. P. Barabashov, G. B. Gumenchuk, M. K. Beyer, A. N. Ponomaryov, and V. E. Bondybey, J. Phys. Chem. A 119, 2475 (2015).
- ¹⁸E. V. Savchenko, I. V. Khyzhniy, S. A. Uyutnov, M. A. Bludov, A. P. Barabashov, G. B. Gumenchuk, and V. E. Bondybey, J. Low Temp. Phys. 187, 62 (2017).
- ¹⁹E. V. Savchenko, I. V. Khyzhniy, S. A. Uyutnov, M. A. Bludov, A. P. Barabashov, G. B. Gumenchuk, and V. E. Bondybey, J. Lumin. 191, 73 (2017).
- ²⁰E. V. Savchenko, I. V. Khyzhniy, S. A. Uyutnov, and M. A. Bludov, Fiz. Nizk. Temp. **50**, 93 (2024) [Low Temp. Phys. **50**, 89 (2024)].
- 21 E. B. Gordon, L. P. Mezhov-Deglin, and O. F. Pugachev, JETP Lett. 19, 63 (1974).
- ²²E. B. Gordon, L. P. Mezhov-Deglin, O. F. Pugachev, and V. V. Khmelenko Cryogenics 16, 555 (1976).
- 23 E. B. Gordon, V. V. Khmelenko, A. A. Pelmenev, and O. F. Pugachev, Physica 108, 1311 (1981).
- 108, 1311 (1981).

 24 E. B. Gordon, A. A. Pelmenev, O. F. Pugachev, and V. V. Khmelenko, Chem Phys. 61, 35 (1981).
- ²⁵R. E. Boltnev, E. B. Gordon, V. V. Khmelenko, I. N. Krushinskaya, M. V. Martynenko, A. A. Pelmenev, E. A. Popov, and A. F. Shestakov, Chem. Phys. 189, 367 (1994).
- ²⁶R. E. Boltnev, I. N. Krushinskaya, A. A. Pelmenev, D. Y. Stolyarov, and V. V. Khmelenko, Chem. Phys. Lett. 305, 217 (1999).
- V. V. Khmelenko, I. N. Krushinskaya, R. E. Boltnev, I. B. Bykhalo,
 A. A. Pelmenev, and D. M. Lee, Fiz. Nizk. Temp. 38, 871 (2012) [Low Temp.
 Phys. 38, 688 (2012)].
 V. V. Khmelenko, A. A. Pelmenev, I. N. Krushinskaya, I. B. Bykhalo,
- ²⁸V. V. Khmelenko, A. A. Pelmenev, I. N. Krushinskaya, I. B. Bykhalo R. E. Boltnev, and D. M. Lee, J. Low Temp. Phys. 171, 302 (2013).
- ²⁹A. Meraki, S. Mao, P. T. McColgan, R. E. Boltnev, D. M. Lee, and V. V. Khmelenko, J. Low Temp. Phys. 185, 269 (2016).
- ³⁰P. T. McColgan, A. Meraki, R. E. Boltnev, D. M. Lee, and V. V. Khmelenko, J. Phys. Chem. A **121**, 9045 (2017).
- ³¹P. T. McColgan, A. Meraki, R. E. Boltnev, S. Sheludiakov, D. M. Lee, and V. V. Khmelenko, J. Phys. Conf. Ser. 969, 012007 (2018).
- ³²P. T. McColgan, S. Sheludiakov, R. E. Boltnev, D. M. Lee, and V. V. Khmelenko, Chem. Phys. 516, 33 (2019).
- ³³A. Meraki, P. T. McColgan, P. M. Rentzepis, R. Z. Li, D. M. Lee, and V. V. Khmelenko, Phys. Rev. B 95, 104502 (2017).
- ³⁴A. Meraki, P. M. McColgan, S. Sheludiakov, D. M. Lee, and V. V. Khmelenko, Fiz. Nizk. Temp. 45, 862 (2019) [Low Temp. Phys. 45, 737 (2019)].
- ³⁵P. T. McColgan, S. Sheludiakov, P. M. Rentzepis, D. M. Lee, and V. V. Khmelenko, Fiz. Nizk. Temp. 45, 356 (2019) [Low Temp. Phys. 45, 310 (2019)].

- ³⁶C. K. Wetzel, D. M. Lee, and V. V. Khmelenko, J. Low Temp. Phys. 215, 294
- (2024).

 37 A. A. Radzig and B. M. Smirnov, Reference Data on Atoms, Molecules, and Ions

 1. Dealin Heidelberg New York, Tokyo, 2012).
- (Springer Science Business Media, Berlin, Heidelberg, New York, Tokyo, 2012). ³⁸R. H. Garstang, "Transition probabilities in auroral lines," in *Airglow and* Auror (Pergamon, New York, 1956), pp. 324–327.

 39A. Lofthus, and P. H. Krupenie, JPCRD 113, 117 (1977).
- 40 E. P. Bernard, R. E. Boltnev, V. V. Khmelenko, and D. M. Lee, J. Low Temp. Phys. 134, 199 (2004).
- ⁴¹S. Mao, R. E. Boltnev, V. V. Khmelenko, and D. M. Lee, Fiz. Nizk. Temp. 38, 1313 (2012) [Low Temp. Phys. 38, 1037 (2012)].
- 42 V. Kiryukhin, B. Keimer, R. E. Boltnev, V. V. Khmelenko, and E. B. Gordon, Phys. Rev. Lett. 79, 1774 (1997).

- 43 V. Kiryukhin, E. P. Bernard, V. V. Khmelenko, R. E. Boltnev, N. V. Krainyukova, and D. M. Lee, Phys. Rev. Lett. 98, 195506 (2007).
- 44N. V. Krainyukova, R. E. Boltnev, E. P. Bernard, V. V. Khmelenko, D. M. Lee, and V. Kiryukhin, Phys. Rev. Lett. 109, 245505 (2012).
- 45 S. I. Kiselev, V. V. Khmelenko, and D. M. Lee, Fiz. Nizk. Temp. 26, 874 (2000)
- J. Low Temp. Phys. 119, 357 (2000).
- ⁴⁷S. I. Kiselev, V. V. Khmelenko, and D. M. Lee, J. Low Temp. Phys. **121**, 671 (2000). 48 V. V. Khmelenko, S. Mao, A. Meraki, S. C. Wilde, P. T. McColgan,
- A. A. Pelmenev, R. E. Boltnev, and D. M. Lee, Phys. Rev. Lett. 111, 183002 (2013).
 ⁴⁹K. Dressler, O. Oehler, and D. A. Smith, Phys. Rev. Lett. 34, 1364 (1974).